Predicting terrestrial gravity noise in the Virgo detector based on new data from site characterization

Susan M. Blackburn
Columbia University, New York, New York 10027, USA
European Gravitational Observatory (EGO), I-56021 Cascina, Pisa, Italy

Characterization of terrestrial gravity (Newtonian) noise in the Virgo detector represents an important preliminary step in developing a predictive model designed to filter this noise from the interferometer's output signal. Seismometer and accelerometer arrays placed in and around Virgo's West End Building in June and July 2016 yielded data that were analyzed with the aim of gathering information about the seismic waves responsible for Newtonian noise effects on the test masses. Following some additional investigations, several persistent spectral lines in the 10 to 20 Hz frequency band were identified and excluded as sources of Newtonian noise. Construction of a model, combining the results of the analysis and structural details of the laboratory buildings and near-surface geology at the Virgo site, is planned. This model will not only allow us to predict and eliminate the spectrum of terrestrial gravity noise in the Virgo detector, but will also contribute to the development of Newtonian noise mitigation schemes in proposed ground-based interferometers.

I. INTRODUCTION

Gravitational waves (GWs) are perturbations in the space-time metric that propagate at the speed of light from high-energy astrophysical events such as the coalescence of compact binary objects. Measuring the mass distortions produced by these waves represents a technological challenge due to the relative weakness of the gravitational force. While Hulse and Taylor achieved indirect detection of GWs in 1975 by measuring the periodic variation of a pulsar in a binary system [1], direct detection has been the decades-long goal of intensive efforts to develop laser interferometry. The successful detection of GWs in 2015 by the Laser Interferometer Gravitational-Wave Observatory (LIGO) experiment in the United States has confirmed the viability of ground-based interferometry in the 10^1 to 10^4 Hz range, and has opened an important new window on astrophysical observation. Efforts are now under way to improve the sensitivity of detectors such as LIGO and Virgo (located near Pisa, Italy) which are limited by various sources of noise in the low-frequency band. Among these, Newtonian noise (NN), is currently of interest in the 10 to 20 Hz range, and may limit sensitivity down to 5 Hz. NN can result from variations in atmospheric pressure or from seismic motion in the medium (soil or rock) surrounding the detector. Seismic waves, particularly those propagating along the surface, can vary the density of this medium, translating to fluctuations in the local gravitational field which couple directly to the test masses. Moreover, these surface waves are subject to scattering and reflection, and can interact with a detector's structural components, generating complex effects. Since shielding from NN is not possible, the implementation of an accurate filtering model of the seismic wave field is necessary. The balance of this paper will present recent efforts to characterize NN at the Virgo detector.

II. NEWTONIAN NOISE

The following subsections provide background on the seismic origins of NN, its mathematical expression, and a brief look at the effects of NN on an interferometer test mass.

A. Seismic motion

Seismic motion represents the dominant source of NN in gravitational wave detectors. While direct mechanical coupling of seismic vibrations to optical components can occur, seismic motion also produces changes in the density of the soil under and around the interferometer, affecting the local value of gravitational acceleration (g), and producing fluctuating Newtonian forces on the suspended test masses.

Seismic waves can be categorized as either surface or body waves. Surface waves travel through the Earth's crust at a lower frequency than body waves, and are responsible for much of the destruction resulting from seismic events. Of particular interest to studies of NN are surface Rayleigh waves (fig. 1), which dominate in the 10 to 20 Hz regime. These have a rolling, elliptical motion with an amplitude that falls off exponentially as a function of depth, producing an evanescent extension of the displacement field [2]. The retrograde particle motion of the Rayleigh wave is limited to the vertical plane in the direction of propagation. This displacement in the normal direction causes a decrease in density of air pockets in the soil, and a corresponding increase in the density of the surrounding soil medium. While precise wave speed is determined by wave frequency and wavelength, Rayleigh waves travel at approximately 300 m/s, and are subject to dispersion and reflection from topography and other obstacles.

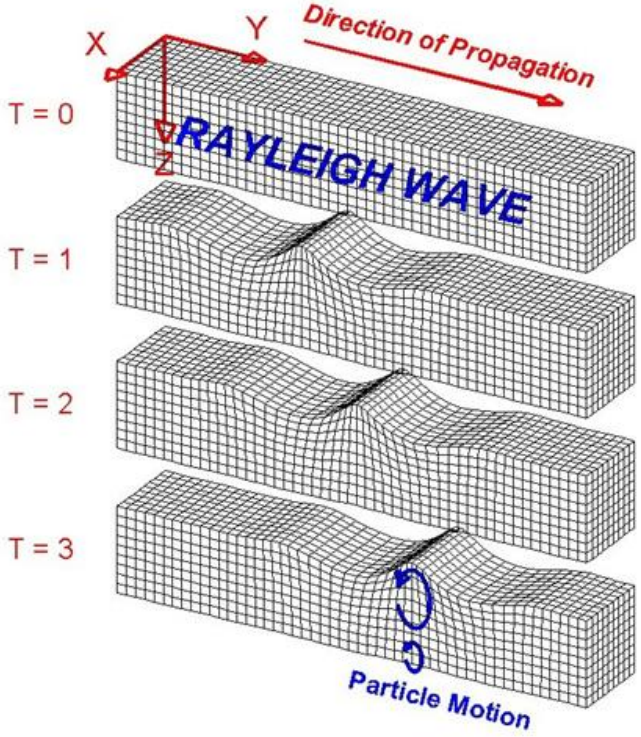

FIG. 1: Rayleigh wave depicted traveling through medium, with particles represented by cubes. Note retrograde particle motion responsible for soil density fluctuations.

In contrast, body waves, which are characterized by a constant amplitude, propagate from sources more distant and deeper underground, and can travel in three dimensions. Two types exist: compressional, or P waves, and shear, or S waves. While compressional wave speed is approximately 320 m/s, shear waves can travel at approximately 600-700 m/s. It is important to note that P waves, like Rayleigh waves, can cause compression and dilation of the ground beneath the surface. While S waves in the medium do not produce any density perturbation, they can displace surface and compressional waves, resulting in some cancellation between wave types.

B. Mathematical description of Newtonian noise

The steady-state process of compression and expansion of soil mass within a system dictates that we can describe seismic motion with a continuity equation since mass is effectively conserved

$$\frac{\partial \rho}{\partial t} + \nabla \cdot \mathbf{j} = 0 \tag{1}$$

where $\mathbf{j}$ represents soil flux in kg $m^{-2}s^{-1}$.

From the continuity equation we can derive the perturbation of soil density as a result of seismic motion [3], which is given by

$$\delta\rho(\mathbf{r},t) = -\nabla \cdot (\rho(\mathbf{r})\vec{\xi}(\mathbf{r},t)) \tag{2}$$

where $\mathbf{r}$ is the position vector, and $\vec{\xi}(\mathbf{r},t)$ represents the seismic wave field.

A corresponding equation for the resulting perturbation of gravity potential in the interferometer test masses follows:

$$\delta\phi(\mathbf{r}_o,t) = G\int dV\rho(\mathbf{r})\vec{\xi}(\mathbf{r},t)\cdot\frac{\mathbf{r}-\mathbf{r}_0}{|\mathbf{r}-\mathbf{r}_0|^3} \tag{3}$$

In a homogeneous medium, separate equations for bulk and surface contributions can often simplify calculations. The expression for the bulk term is

$$\delta\phi_{bulk}(\mathbf{r}_o,t) = G\rho_0\int_\nu dV\frac{\nabla\cdot\vec{\xi}(\mathbf{r},t)}{|\mathbf{r}-\mathbf{r}_0|} \tag{3.1}$$

and for the surface term is

$$\delta\phi_{surface}(\mathbf{r}_o,t) = -G\rho_0\int dS\frac{\mathbf{n}(\mathbf{r})\cdot\vec{\xi}(\mathbf{r},t)}{|\mathbf{r}-\mathbf{r}_0|} \tag{3.2}$$

C. Effects of Newtonian noise on an interferometer test mass

An interferometer test mass is suspended freely above a medium (fig. 2)[4]. Using an *xyz* coordinate system we locate the mirror at $\mathbf{y}$. A volume dV of soil at $\mathbf{r}$ undergoes a seismic displacement ($\mathbf{r}$, t). The medium has an equilibrium density of $\rho_0(\mathbf{r})$ and an instantaneous density $\rho(\mathbf{r},t) = \rho_0(\mathbf{r}) + \delta\rho(\mathbf{r},t)$ caused by the seismic displacement field. The position of dV with respect to the test mass is given by $\mathbf{r\prime} = \mathbf{r} - \mathbf{y}$. A Newtonian acceleration $\mathbf{a}(\mathbf{y},t)$ acts on the test mass and is comprised of a static contribution $\mathbf{a}_{static}(\mathbf{y})$ plus a Newtonian noise contribution $\delta\mathbf{a}_{NN}(\mathbf{y},t)$ due to the seismic density fluctuations.

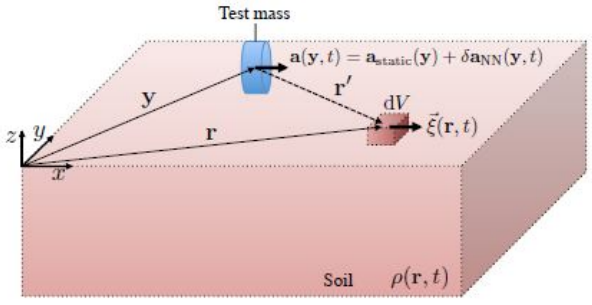

FIG. 2: Schematic showing mathematical description of NN effects on interferometer test mass suspended above soil medium.

III. WEST END BUILDING ENVIRONMENT

Since seismic surface waves have the potential to be scattered and reflected by an interferometer's structural components, building characteristics become a key consideration in producing an accurate NN profile. It is valuable therefore to examine environmental features that might contribute to or otherwise alter these effects. At Virgo, both West and North End Buildings are effectively identical in construction and layout, so it is reasonable to infer that site studies conducted at one are applicable to the other. The West End Building (WEB) was chosen for data-taking due to ongoing commissioning activities in the North End Building.

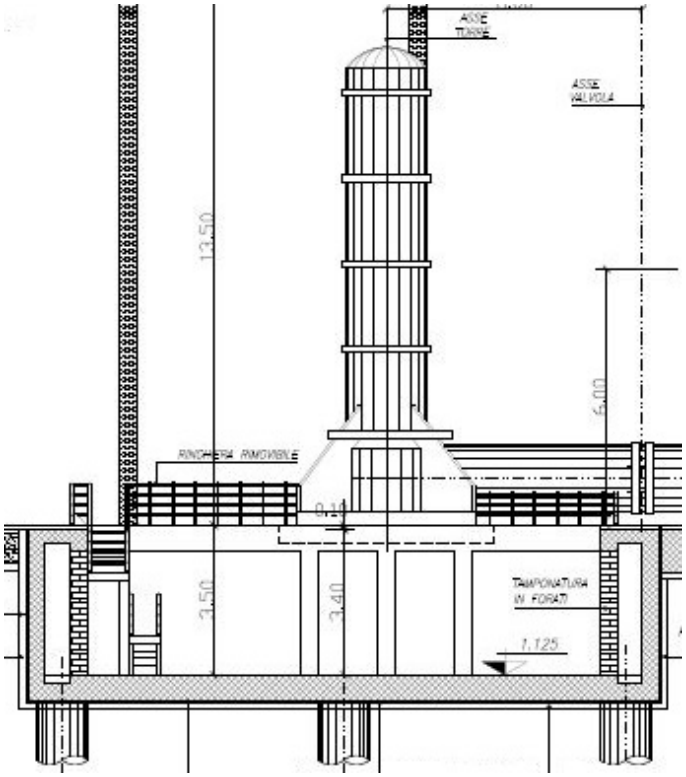

FIG. 3: Technical drawing showing Virgo's West End Building (WEB) tower in profile. Note basement room extending beneath tower and supporting piles.

The WEB is constructed of two independent concrete slabs. The inner slab, 6 m wide and 15 m long supports the vacuum tank (hereinafter referred to as the "tower") which hosts the mirror test mass suspension. It is important to note that unlike LIGO's simple slab design, Virgo's tower construction includes a clean room basement (fig. 3), consisting of a hollow space cut into the concrete slab, which is used for payload installation. The tower floor sits on piles 1200 mm in diameter that penetrate the soil to reach the compact and stable gravel layer located 52 m beneath the surface, and is separated by a 5 cm gap from the outer floor in order to improve isolation with respect to vibrations of the building. The outer slab supports the building's external concrete shell and is supported by piles sitting at a reduced depth on the softer clay soil.

At the western extremity of the tower building are appended technical rooms hosting the 15 kV power connection, transformers, uninterrupted power supplies, a diesel generator, and pumps for chilled and hot water circulation to the HVAC. These sit on a third concrete layer resting on the soil surface with no supporting piles.

IV. SEISMIC FIELD CHARACTERIZATION

Investigations of the seismic field in and around the WEB were carried out in June and July 2016, and are described in the following subsections.

A. Comparative seismicity inside and outside the West End Building

Relative levels of seismicity between the WEB tower floor and exterior environment were investigated by deploying two triaxial low-frequency Nanometrics Trillium C20 velocimeters, with a measuring range of 0.1 Hz to 50 Hz. The indoor sensor was placed on the tower floor, to the east of the tower, and the outdoor sensor placed south of the WEB parking lot (fig. 4).

FIG. 4: Aerial view of Virgo's West End Building showing approximate locations of outdoor and indoor sensors.

Distance between the two sensors was approximately 35 m. Signal was output to a Nanometrics Centaur digital datalogger with 24-bit ADC, GPS antenna receiver and 16 GB removable SD card. Dynamic range for the indoor sensor was 40 V, and for the outdoor sensor 4 V, with both sensors sampling at 250 Hz. Both sensors were powered by rechargeable 12 V batteries. Data were taken from June 9, approximately 11:00 UTC, to June 15, approximately 14:00 UTC. Vacuum pumps on and around the tower were switched off on Sunday June 12 for most of the day, replicating "science mode" conditions when the WEB is restricted to human and vehicle

traffic. Approximately 24 hours of data were analyzed from this period, and seismic spectra were produced as shown in fig. 5 and 6 below.

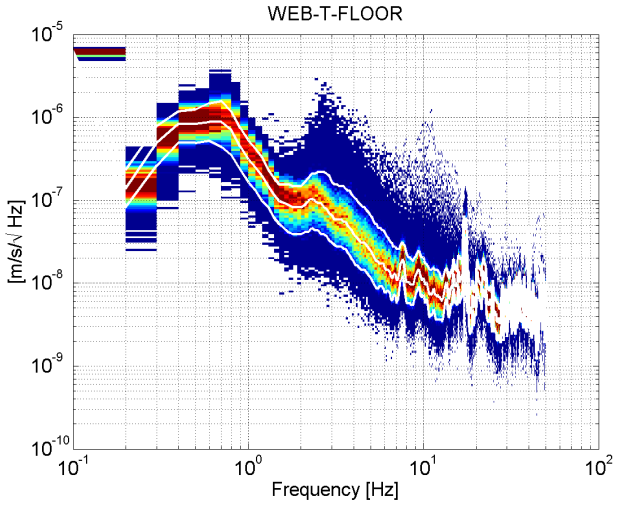

FIG. 5: Seismic spectrogram showing 10th, 50th and 90th percentiles for interior (tower floor) sensor.

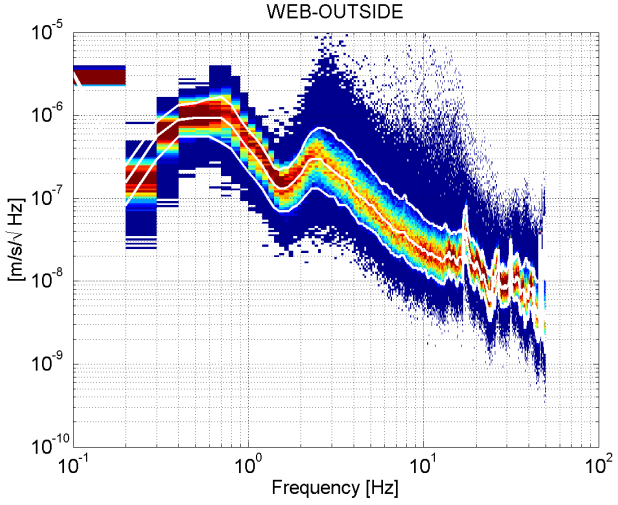

FIG. 6: Seismic spectrogram showing 10th, 50th and 90th percentiles for exterior sensor

A comparison of the two median, or 50th percentile, spectra (fig. 7) confirms that the tower floor is seismically quieter than the exterior of the WEB by approximately a factor of three, beginning from about 2 Hz. This result is not unexpected given that the tower is effectively "moated" by a gap between it and the building slab, as explained previously.

At approximately 17 Hz and 20-25 Hz it was noted that seismic noise is the same both inside and outside the WEB. This prompted further investigation of potential local noise sources, which is discussed in detail later in this paper.

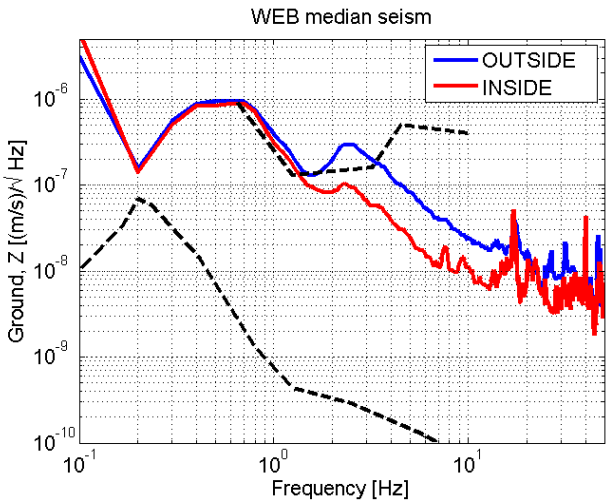

FIG. 7: Comparison of 50th percentile spectra for indoor and outdoor sensors. Dashed lines show highest and lowest levels of observed seismic noise at "seismically-quiet" sites, based on the USGS Peterson model (1993).

B. Seismicity within the West End Building

Three accelerometer arrays in configurations parallel to the interferometer arm (z-array) perpendicular to the arm (x-array) and in a circle surrounding the tower (c-array) were used to investigate seismicity within the WEB. Array configurations and sensor locations are shown in fig. 8 below.

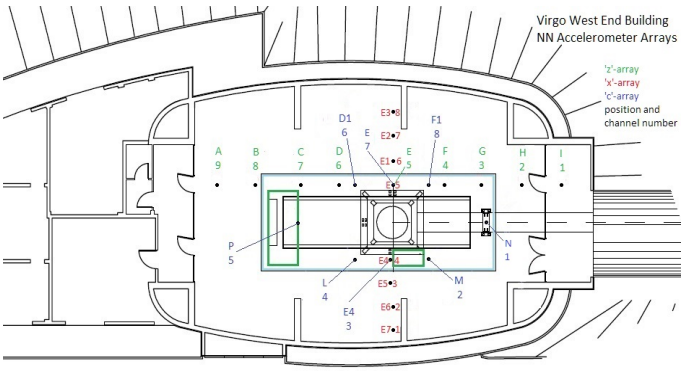

FIG. 8: Location and placement of z, x and c accelerometer arrays on Virgo's WEB floor.

All arrays were placed symmetric with respect to the axis suggested by the direction of the arm, and all sensors were located at a distance from the test mass representing a fraction of the seismic wavelength of interest in order to avoid diminishing correlation with NN due to limitations of sensor signal-to-noise ratio.

Wilcoxon Meggit-731 single-axis (vertical) accelerometers with sensitivity 1 V/g were employed in these investigations. Sensors were positioned vertically and fixed to the painted concrete floor with double-sided tape (fig. 9).

FIG. 9: Wilcoxon Meggit-731 accelerometer affixed to WEB floor

The sensors were powered with Wilcoxon P703B power units, and data were output to the WEB ADC channels. Eight sensors were used in the x and c-arrays with one additional sensor (PCB-393B12) employed in the z-array.

Data were taken over three successive weekends in order to reduce the incidence of anthropogenic noise from activity in and around the tower and WEB environs. Dates of data-taking for z-array were June 10-13, x-array June 17-20, and c-array June 24 to 27.

To evaluate the performance of the sensors and cabling, and to identify any equipment faults, a huddle test was conducted on the WEB floor on June 24, resulting in the amplification of one sensor by a factor of 10.

An intrinsic noise budget for the accelerometers and ADC (z-array configuration) is plotted in fig. 10, and demonstrates a signal-to-noise ratio on the tower floor of approximately order 10.

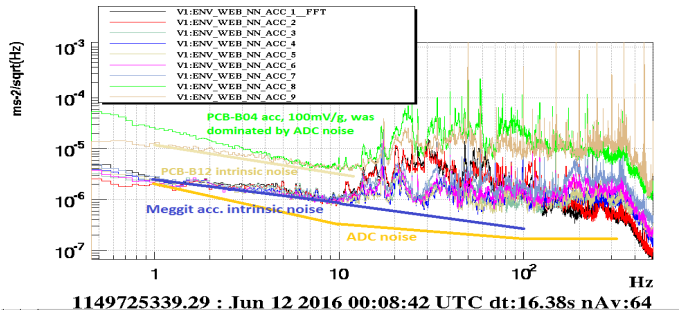

FIG. 10: Accelerometer noise budget (z-array) indicating intrinsic sensor and ADC noise.

48 hours of averaged data from the z-array confirmed that the tower floor is seismically quieter than the building floor as evidenced by the comparison plot of median spectra for sensors on and off the tower floor (fig. 11). In the region of interest between 10 and 20 Hz, a mysterious peak persists at 17 Hz.

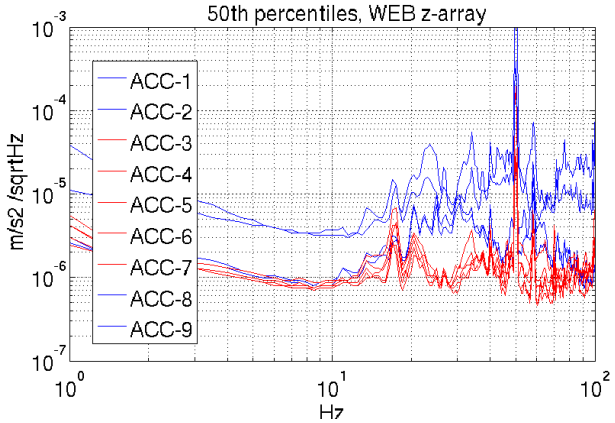

FIG. 11: Comparison of median spectra of z-array tower floor accelerometers (shown in red) and building floor accelerometers (shown in blue). Note 17 Hz peak.

A similar result was obtained from x-array data (fig. 12), which also shows a lower noise level on the tower floor. This suggests again that the tower-platform interface is responsible for a mechanical filtering effect.

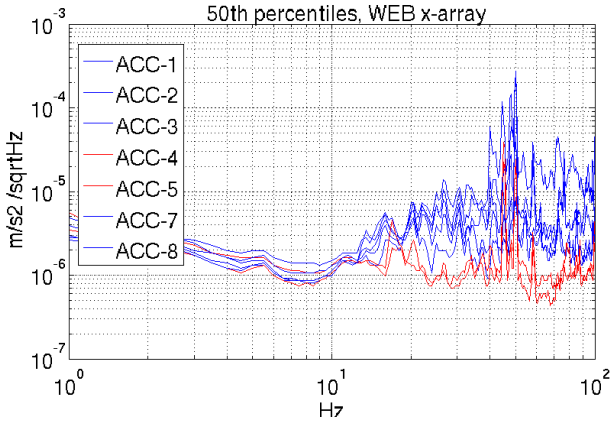

FIG. 12: Comparison of median spectra of x-array tower floor accelerometers (shown in red) and building floor accelerometers (shown in blue).

It is worth noting that the noise contributions from a vacuum scroll pump located on the tower floor were eliminated from this analysis by choosing data taken during times that this pump was switched off, as it would be during science mode.

It was also seen that the 17 Hz peaks first identified by the interior-exterior array persisted in data collected in the z and x-arrays. In addition, bumps at 12 Hz, and a modulated line between approximately 17.5 and 20.5 Hz were noted and subsequently investigated. Details of these investigations are described below.

Following from the conclusion that the WEB tower floor is, relatively speaking, a seismically quiet environment, comparison plots (fig. 13 and 14) between noise on the Virgo WEB tower floor and at LIGO Hanford and LIGO Livingston sites were produced using data from the interior Trillium seismometer.

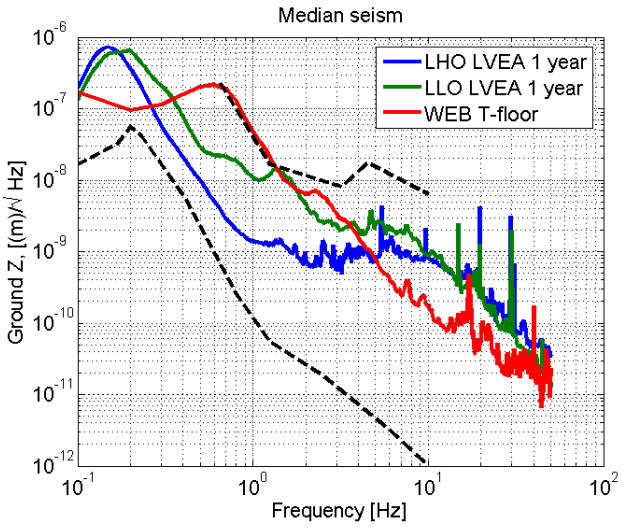

FIG. 13: Comparison of median seism between Virgo tower floor (red), LIGO Hanford (blue) and LIGO Livingston (green) in units of displacement.

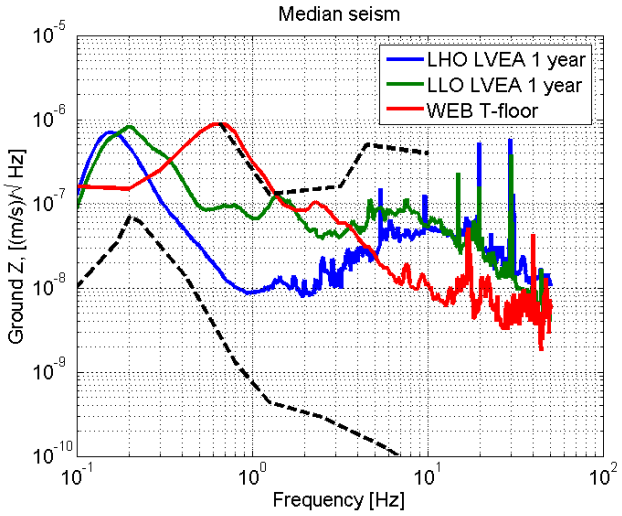

FIG. 14: Comparison of median seism between Virgo tower floor Red), LIGO Hanford (blue) and LIGO Livingston (green) in units of velocity.

Our analysis revealed that between 5 and 20 Hz, Virgo's tower floor is seismically quieter than both LIGO sites. Again it is a reasonable assumption that the interface between the tower floor and building floor (absent at both LIGO sites) is acting as a filtering mechanism, and suggests that seismic waves may be reflected from it.

The focus of our efforts shifted to hunting for the sources of spectral lines in order to rule these out at NN sources. Directional analysis was undertaken in order to try to determine the direction and speed of the seismic wave field at 12 Hz and 17 Hz. Histograms produced showing z-array seismic spatial spectra at 12 and 17 Hz were plotted (fig. 15):

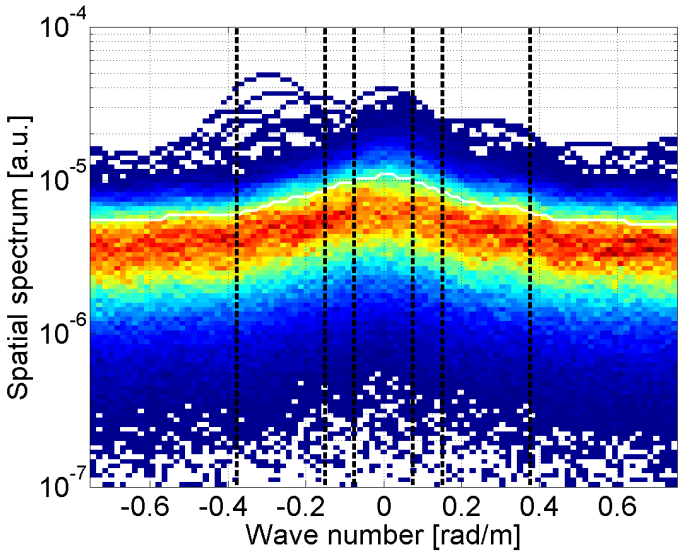

(a)

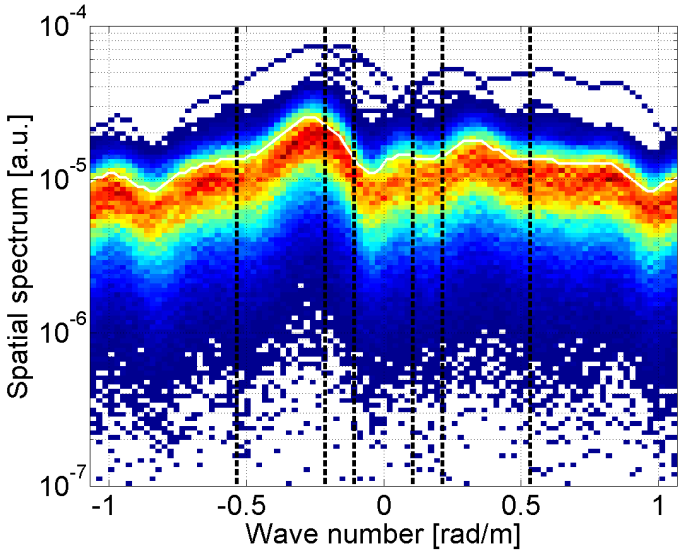

(b)

FIG. 15: Histograms of seismic spatial spectra for z-array at (a) 12 Hz, and (b) 17 Hz.

Wavenumber is plotted on the x-axis, with sign indicating direction. Wavenumbers can be translated into seismic speeds since these spatial spectra are evaluated at specific temporal frequencies (12Hz, and 17Hz). The dashed vertical lines from left to right correspond to seismic speeds -200, -500, -1000, 1000, 500, and 200 m/s

respectively.

At 12Hz the seismic energy is in high-speed waves, while at 17Hz, the maximum amplitude is at about -350 m/s, suggesting that the wave comes from the direction of the corner station. However, since the array is 1D, this result is inconclusive.

It is likely, based on previous seismic studies of the area surrounding the Virgo site (see https://tds.ego-gw.it/itf/tds/index.php?callContent=2callCode=1463), that the 12 Hz line is due to automobile and truck traffic over local bridges.

Adopting this as a reasonable hypothesis, we proceeded with a systematic hunt for the unidentified noise sources. We switched off and back on several mechanical components in the WEB while the c-array was deployed and taking data. These components are indicated in the map below (fig. 16)

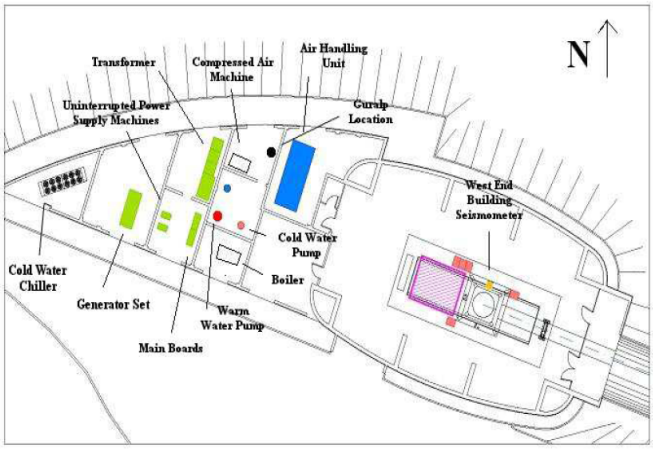

FIG. 16: Map of Virgo's WEB infrastructure components.

By switching off the air conditioner, and hot and cold water pumps we saw a clear reduction in noise in the 20 to 30 Hz range (fig. 17)

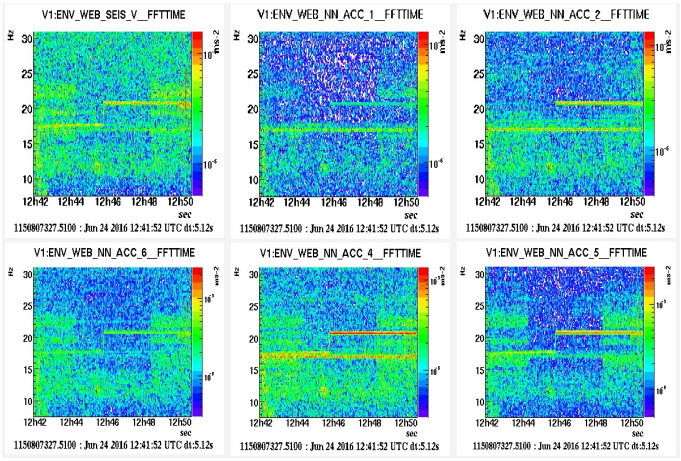

FIG. 17: Spectrogram showing reduction of noise in 20 to 30 Hz range due to WEB mechanical component switching tests with c-array sensors active.

Switch on and off times of the cold water pump corresponded closely to the noise reduction in this range. Further switching tests of the air compressor, heater and chiller were undertaken to eliminate the uncertainty surrounding the variable noise at 17.5 to 20.5 Hz (fig. 18). Unfortunately no conclusive results were obtained.

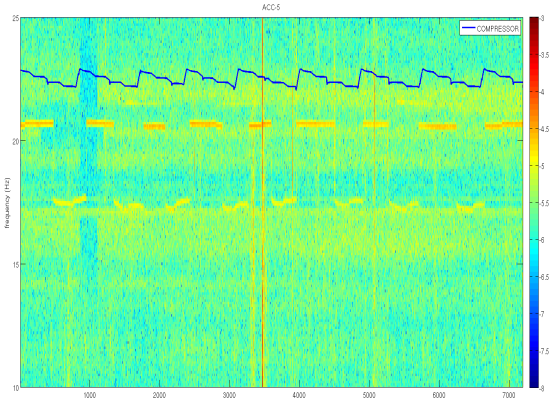

FIG. 18: Spectrogram showing persistent modulated line between 17.5 and 20.5 Hz.

Five sensors were then placed the walls of the structure housing the suspended bench (SWEB) at the end of the west arm. Here, by performing a similar switching test, it was conclusively determined that cooling fans on top of the structure are the source of the 17 Hz line (fig. 19).

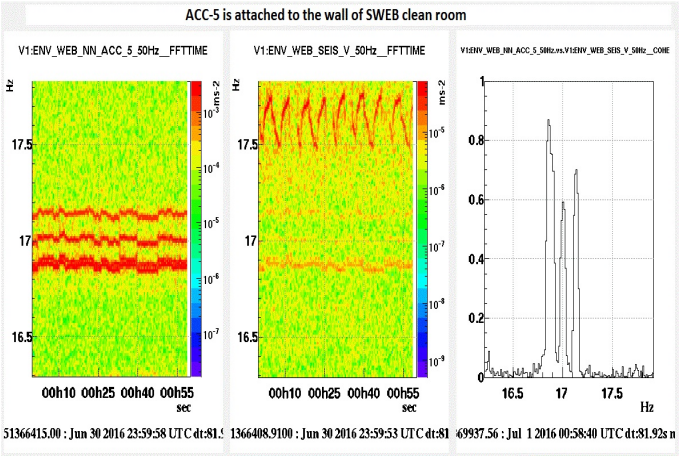

FIG. 19: SWEB fans clearly identified as source of 17 Hz spectral line.

C. Miscellaneous Noise-Hunting Tests

Further investigations were carried out using a single accelerometer and a portable spectrum analyzer to attempt to determine the source of the modulated noise jumping between 17.5 and 20.5 Hz. We observed that the signal amplitude increases approaching the technical rooms hosting the mechanical infrastructure and found it to be loudest close to the wall separating the water pumps and the air conditioning unit. An examination of data from the Trillium sensors used in the indoor-outdoor noise tests revealed that this line has virtually equal amplitude at both interior and exterior (fig. 20) sensor locations, and appears also on spectra from the permanent episensor located on the tower platform. Efforts are ongoing to identify the source of this line.

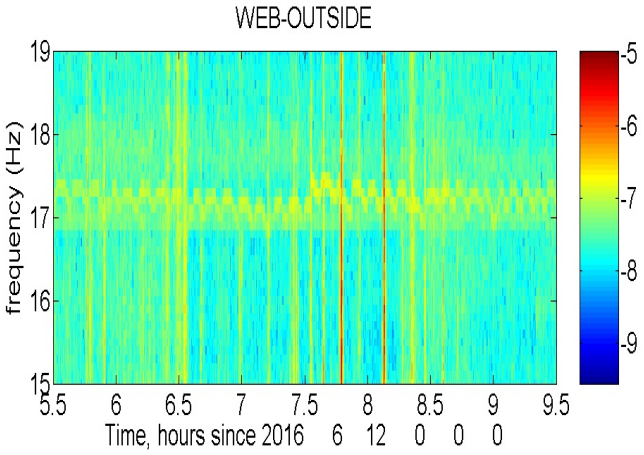

FIG. 20: Exterior Trillium sensor showing modulated line in 17.5 to 20.5 Hz range.

D. Seismometer WEB Tower Floor Correlation Test

The correlation properties of seismic motion are not only important to our understanding of the impact of NN on test masses, but also for optimizing the sensor arrays designed to cancel out this noise.

Correlation describes the degree to which two signals are in phase. When they are perfectly in phase, the correlation is 1, whereas if they are 180 degrees out of phase, the correlation is -1.

Coherence is a measure of similarity between two signals, and describes how closely the signals would resemble each other under a linear transformation in time. This means that if one seismic signal can be obtained from a linear transformation of the other, the coherence is equal to one. Completely unrelated signals have a coherence of zero.

A largely coherent soil mass will require a less dense array of sensors, whereas relatively incoherent ground will need a larger number of sensors placed more closely together.

Correlation tests were performed on the tower floor by fixing the location of one Trillium sensor, while placing a second sensor at consecutively increasing distances. Distances of 2, 7 and 9 meters were chosen. Plots for each are displayed below in fig. 21, 22, and 23:

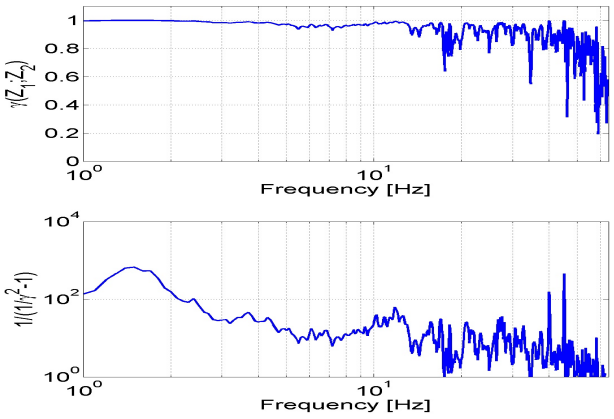

FIG. 21: WEB tower floor correlation test at distance 2 m.

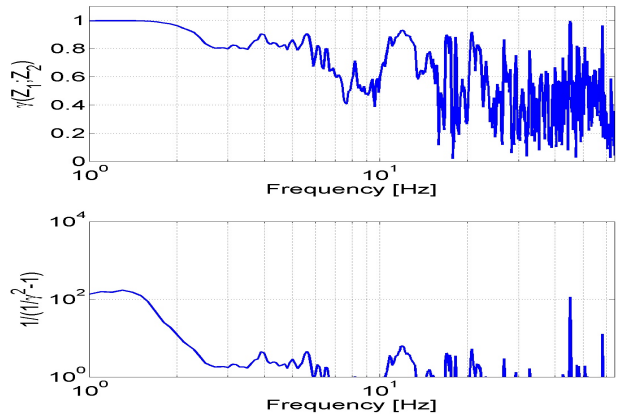

FIG. 22: WEB tower floor correlation test at distance 7 m.

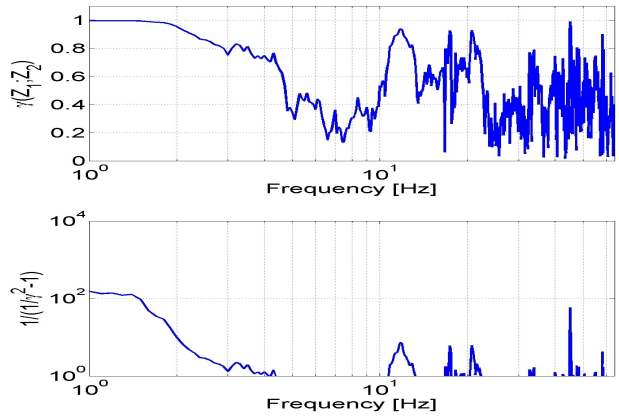

FIG. 23: WEB tower floor correlation test at distance 9 m.

It appears that while a component of the seismic field has a short correlation length, there is a component at approximately 11 Hz that maintains correlation over longer distances. It is hypothesized that this component could be due to an independent wave source below 10 Hz. It could also indicate different sources on or off the tower platform, or wave propagation through the supporting piles of the tower. This suggests once again that Virgo's seismic environment is unexpectedly complex and warrants more detailed study.

IV. CONCLUSIONS

Several local noise sources in 10-20 Hz band, not all of which have been identified, contribute to the complexity of Virgo's NN profile. This suggests that existing NN cancellation models, such as have been developed at LIGO Hanford, are too simple in their current form to implement at Virgo, and will require much more extensive development to be used effectively.

Similarly, structural components in Virgo's WEB, primarily the basement clean room and building-tower interface, are causing scattering and reflection of seismic waves, again making existing NN cancellation models difficult to implement. This is in contrast to the relatively simple situation at LIGO, where the interferometer sits on a simple concrete slab.

Finally, correlation lengths are quite short at Virgo as evidenced from our tests, and therefore an optimized sensor array will require a small diameter and very precise sensor placement.

It is hoped that ongoing efforts to develop more sophisticated models will enable the accurate prediction of NN and its subtraction from the Virgo interferometer output signal.

ACKNOWLEDGEMENTS

I am grateful to the National Science Foundation for supporting my participation in the University of Florida's IREU program in Gravitational Physics. I thank my advisors, Dr. Irene Fiori, Dr. Jan Harms, and Dr. Giancarlo Cella for generously sharing their time and expertise. Thanks also to many others at EGO for contributing technical and practical assistance, and for extending kindness and hospitality during my stay. Finally, I would like to thank the organizers of the IREU program for making this outstanding opportunity possible.